NOVA SCHOOL OF SCIENCE & TECHNOLOGY

DEPARTAMENT OF MATERIALS SCIENCE

MARGARIDA MACHADO DA GRAÇA PAES AFONSO

BSc in Materials Engineering Science

Stable structural colour patterns displayed on transparent cellulose composite free-standing films

MASTER IN MATERIALS ENGINEERING

NOVA University Lisbon

September 2023

NOVA SCHOOL OF SCIENCE & TECHNOLOGY

DEPARTAMENT OF
MATERIALS SCIENCE

STABLE STRUCTURAL COLOUR PATTERNS DISPLAYED ON TRANSPARENT CELLULOSE COMPOSITE FREE-STANDING FILMS

MARGARIDA MACHADO DA GRAÇA PAES AFONSO

BSc in Materials Engineering Science

Adviser: Doctor Maria Helena Figueiredo Godinho
Associate Professor with Habilitation, NOVA University Lisbon

Co-adviser: Doctor Pedro Marques de Almeida
Associate Professor with Habilitation, NOVA University Lisbon

Examination Committee:

Chair: Prof. Dr^{o} João Paulo Borges

Rapporteurs: Prof. Dr^{a} Ana Almeida

Adviser: Prof. Dr^{o} Pedro Marques de Almeida

Members:

MASTER IN MATERIALS ENGINEERING

NOVA University Lisbon
September 2023

Stable structural colour patterns displayed on transparent cellulose composite free-standing films

Aos meus queridos pais.

AGRADECIMENTOS

Em primeiro lugar, gostaria de agradecer à minha querida NOVA FCT e ao DCM, por terem sido a minha casa nos últimos 5 anos. A todos os Professores que, em tempos de mudança e mais dificuldade, se adaptaram para nos continuar a proporcionar um excelente ensino à distância.

À minha orientadora, Professora Doutora Maria Helena Godinho, por todos os ensinamentos e ajuda disponibilizada durante estes cinco anos, por me despertar um especial interesse por esta área e, em especial, durante o decorrer da dissertação, por todas oportunidades e experiência que me permitiu usufruir. Ao meu coorientador, Professor Doutor Pedro Almeida, pela sua ajuda incansável, disponibilidade, paciência e compreensão durante estes meses de trabalho, por todo o apoio e incentivo que ajudaram a tornar esta fase mais serena.

Agradeço profundamente ao Professor José Paulo Farinha e ao Instituto Superior Técnico, por me permitirem utilizar as instalações e equipamentos cruciais para a obtenção de dados nesta dissertação. Agradeço também ao Doutor Roberto Keller e ao Museu Nacional de História Natural e da Ciência, pela ajuda na identificação da espécie e pelas valiosas fotografias que contribuíram significativamente para este trabalho.

A todos os meus queridos amigos, em especial, os *Masqueicos*, pelas memórias, ajuda, amizade, carinho e apoio com o qual moldaram esta experiência que é a Faculdade, e tornaram esta fase da vida tão especial. Por todos os faisões, convívios na Solução, boleias, idas ao Sunrise, jogos de Gartic Phone, partilha de fotografias às quatro da manhã, "estudos" na 203, minifférias e todo o tempo que passámos juntos, obrigada.

Aos meus pais, que me proporcionaram tudo isto (e muito mais!), incentivando e apoiando sempre todos os meus projetos e objetivos, mostrando orgulho nas minhas conquistas e ajudando-me a superar as dificuldades. O seu apoio inabalável, amor e encorajamento foram pilares essenciais ao longo de todo este percurso, e por isso, muito obrigada.

Às minhas irmãs, por todos os conselhos, apoio e ajuda, quer em momentos bons, quer em momentos menos bons. Por me ajudaram a concretizar sonhos e objetivos, por serem modelos inspiradores, confidentes fiéis e apoios incondicionais. Esta jornada não teria sido a mesma sem a vossa ajuda.

Aos meus avós, por todo o carinho e palavras sábias de incentivo, boleias e almoços especiais para a neta preferida.

“Now, this is not the end. It is not even the beginning of the end. But it is, perhaps, the end of the beginning.” (Winston Churchill).

ABSTRACT

Natural structures can generate colours through various mechanisms, such as multilayers and diffraction gratings. For example, the colour patterns observed in the wings of insects result from transparent solid films and are attributed to thin film interference and corrugations resembling fingerprint patterns. These microstructures enhance the wing's interference patterns and reduce iridescence across different angles of light due to the convex ridges.

Conversely, transparent films made from cellulose nanocrystals suspended in water are known for their iridescence and their ability to selectively reflect left circularly polarized light while transmitting right circularly polarized light. Efforts have been made to control their optical properties, including reducing iridescence.

In the present work, the optical properties of thin transparent cellulosic films were combined by creating a banded layer on top of an iridescent CNCs film. The study aimed to explore these films' optical and mechanical characteristics and compare them with those observed in the transparent wings of *Xylocopa violacea*.

However, the results were unexpected. Despite the efforts to control the optical properties and reduce iridescence, the combination of these films did not yield the anticipated improvements. The mechanical characteristics also did not behave as predicted.

In conclusion, while it was hoped to achieve significant progress in enhancing the optical properties of cellulose-based films, the study's unexpected outcomes underscore the complexity of these systems. These findings provide valuable insights for future research, emphasizing the need for more refined approaches and a deeper understanding of these materials. Despite the challenges encountered, the study contributes to the ongoing exploration of thin (~60 μm) transparent cellulose films and their potential applications.

Keywords: Natural structures, Thin films, Cellulose, Iridescence, Nanocrystals, Optical properties, Thin film interference.

RESUMO

Estruturas naturais têm a capacidade de gerar cores através de diversos mecanismos, sendo os mais comuns as multicamadas e as redes de difração. Por exemplo, os padrões de cores que observamos nas asas de insetos, resultantes de filmes sólidos transparentes, são atribuídos à interferência de filmes finos e às corrugações que se assemelham a padrões de impressões digitais. Estas microestruturas aprimoram os padrões de interferência na asa e reduzem a iridescência em diferentes ângulos de luz devido às cristas convexas.

Por outro lado, filmes transparentes feitos a partir de nanocristais de celulose suspensos em água são conhecidos pela sua iridescência e pela capacidade de refletir seletivamente a luz polarizada circularmente à esquerda, enquanto transmitem a luz polarizada circularmente à direita. Vários esforços têm sido feitos para controlar as suas propriedades óticas, incluindo a redução da iridescência.

Neste estudo, as propriedades óticas de filmes finos transparentes de cellulose foram combinadas, criando um filme em faixas sobre um filme iridescente de nanocristais de celulose. O objetivo era explorar as características óticas e mecânicas destes filmes e compará-los com as observadas nas asas transparentes de *Xylocopa violacea*.

No entanto, os resultados foram inesperados. Apesar dos esforços para controlar as propriedades óticas e reduzir a iridescência, a combinação destes filmes não produziu as melhorias esperadas. As características mecânicas também não se comportaram como previsto.

Em conclusão, apesar de o esperado ser alcançar avanços significativos na melhoria das propriedades óticas dos filmes de celulose, os resultados inesperados deste estudo destacam a complexidade destes sistemas. Estas descobertas fornecem informações valiosas para futuras pesquisas, enfatizando a necessidade de abordagens mais refinadas e uma compreensão mais profunda destes materiais. Apesar dos desafios encontrados, este estudo contribui para a exploração contínua dos filmes finos (~60 μm) transparentes de celulose e das suas potenciais aplicações.

Palavras chave: Estruturas naturais, Filmes finos, Celulose, Iridescência, Nanocristais, Propriedades óticas, Interferência de filmes finos.

CONTENTS

LIST OF FIGURES

LIST OF TABLES

ACRONYMS

OH	Hydroxyl groups.
HPC	Hydroxypropyl cellulose.
CNC	Nanocrystalline cellulose.
LCP	Liquid crystalline phases.
LC	Liquid crystalline.
CPL	Circular polarized light.

SYMBOLS

S	The order parameter.
λ	The wavelength.
θ	The angle.
n	The average refractive index.
P	The pitch value.

1

INTRODUCTION

1.1 State of the art

Exploration of colour mechanisms in natural structures reveals the prominence of multilayers and diffraction gratings as key contributors to colour generation [1]. One compelling example lies in the vivid colour patterns emanating from the transparent solid films within insect wings, evidenced in Figure 1.1. These patterns have been attributed to the intricate interplay of thin film interference and corrugated microstructures, reminiscent of fingerprint patterns [2]. These microstructures play a pivotal role in fortifying the wing's interference patterns, leading to the attenuation of iridescence across a range of light incidences. The dioptric stabilisation resulting from convex ridges contributes to this phenomenon, marking a significant step towards minimising the iridescent effects inherent in these structures [3].

Figure 1.1 - Wing Interference Pattern visibility Dynamics. Left: Pigmentation pattern against a reflective white background. Right: WIP reflection against an absorbing black background, adapted from [2].

Moreover, the utility of structural colour in floral morphology has also emerged. Iridescence, a phenomenon traditionally associated with animal species, has now been identified in flowers. This discovery suggests that the presence of iridescence could be more widespread in flowering plants, raising intriguing questions about its ecological implications. While iridescence might heighten visual appeal, its variable appearance from different observer perspectives could potentially compromise accurate target identification.

The realm of cellulose nanocrystals has further enriched our understanding of colour dynamics. Transparent solid free-standing films derived from CNCs aqueous suspensions display distinct iridescence and a unique response to circularly polarised light. These films selectively reflect left circularly polarised light while transmitting right circularly polarised light. With aspirations of harnessing these films for optical applications, substantial efforts have been directed towards modulating their optical properties, particularly their iridescence. This endeavours to position them as promising contenders for innovative optical devices with tailored functionality.

Furthermore, the integration of shear in transparent film fabrication introduces novel dimensions. Films endowed with meticulously engineered surfaces, characterised by periodically distributed bands perpendicular to the shear direction, have been documented. This nuanced surface modulation adds complexity to the field, ushering in the potential to tailor optical and visual properties in innovative and unforeseen ways.

In conclusion, the dynamic interplay between thin film interference, microstructures, and diffraction gratings remains central to the palette of colour generation mechanisms in diverse natural structures. From the captivating patterns adorning insect wings to the burgeoning insights into floral iridescence and the novel realm of cellulose nanocrystal films, along with the creative possibilities of shear modulation, these findings collectively underscore the multidimensional nature of colour phenomena. This richness in understanding paves the way for interdisciplinary exploration and practical applications across a spectrum of scientific domains.

1.2 Cellulose

Cellulose, the most abundant biopolymer on earth, is a biodegradable, renewable, and inexpensive material. These properties make it one of the most studied materials in terms of materials that mimic natural processes. For this reason, and due to the growing concern for the environment and the scarcity of various resources derived from oil, the scientific community has turned to the use of cellulose and its derivatives in various applications. The sources of cellulose include plants, marine animals (tunicates), and bacteria [4].

Cellulose is a main chain organic polymer belonging to the polysaccharide groups. The repetitive unit is cellobiose, which results from the reaction of glucose molecules with the release of water molecules in a polymerization reaction. Cellulose consists of chains of molecules held together by

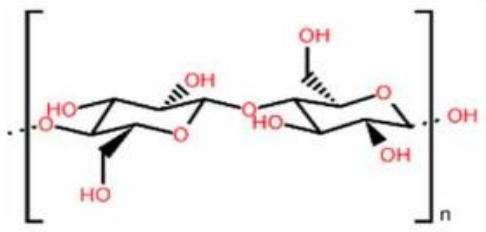

Figure 1.2 - Structure of the cellobiose unit.

intermolecular and intramolecular hydrogen bonds, giving cellulose its flexibility and mechanical strength [4].

Cellulose derivatives are often used, in which the hydroxyl groups (OH) at the C2, C3, and C6 carbon atoms, shown in Figure 1.2, are replaced in a cellobiose unit, which gives cellulose high reactivity. Due to its high reactivity, cellulose can originate cellulose derivatives with different side chains, which translate into the dissolution of polymer in diverse solvents [5,6,7,8].

1.2.1 Hydroxypropyl cellulose

Hydroxypropyl cellulose (HPC) is a commercially available cellulose derivative obtained by replacing on average some of the OH groups on C2, C3, and C6 with an ester functional group, represented in Figure 1.3. HPC aqueous solutions are among the most studied in the literature due to their ability to form lyotropic liquid crystalline phases at room temperature and within a certain range of concentration. Studies show that thin films produced from HPC in aqueous solutions form structures which are similar to liquid crystalline elastomers. Despite some types of HPC being used as film coating polymers, the main application is in the pharmaceutical industry. Due to its deformability and excellent plasticity, HPC is also known as a base material for pharmaceutical films. One of the most appealing properties of HPC as an additive in the pharmaceutical industry, is its solubility in water [8,10,11,12].

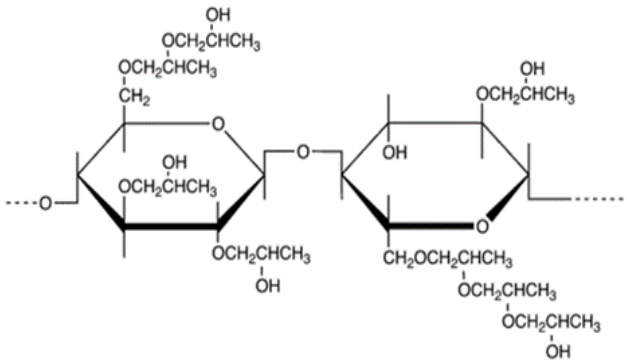

Figure 1.3 - Strucuture of the repetitive unit of HPC [13].

1.3 Nanocrystalline cellulose

Nanocrystalline cellulose, can be isolated from cellulose microfibrils through acid hydrolysis [14]. Acid treatment selectively eliminates the non-crystalline parts of cellulose fibres, resulting in typically rod-shaped rigid nanocrystals [15]. The dimensions, shape, and various properties of CNCs, including their crystallinity level, aspect ratio, and liquid crystalline behaviour, significantly depend on factors such as the source of cellulose, the specifics of the acid hydrolysis process, and subsequent

treatments [11]. CNCs possess outstanding characteristics, including a high Young's modulus, a substantial L/D aspect ratio, leading to a large surface area, hydrophilicity, liquid crystalline behaviour, and low density [16].

1.3.1 Liquid crystalline phases in cellulosic materials and optical properties

Cellulosic materials can form liquid crystalline phases in certain conditions. These phases are also known as mesophases since they present properties of the solids, and the liquids, the molecules do not have a fixed positional order, but present a long-range orientational over distances that are several times longer than the length of the individual molecules. It was found that the cellulosic molecules can self-assemble generating lyotropic and thermotropic liquid crystalline phases. Lyotropic liquid crystalline phases depend on solvent concentration, while thermotropic liquid crystalline phases rely on temperature variations to exhibit distinct molecular arrangements. [8,13,17]

The order parameter, S, is defined to quantify the order present in liquid crystals, where θ is the angle between the director and the major axis of the liquid crystal molecule. and is given by the following equation:

$$S = \frac{1}{2}\langle 3\,cos^2\,\theta - 1\rangle \qquad \text{(Equation 1)}$$

When the liquid crystal molecules are all aligned, we have $\theta = 0$, consequently we have $\langle cos^2\theta\rangle = 1$, so the maximum value of S will be 1 (S=1). On the other hand, when the molecules are randomly distributed, we have the average value $\langle cos^2\theta\rangle = \frac{1}{3}$ giving the minimum value for S, in this case S=0. The order parameter for liquid crystals decreases with increasing temperature.

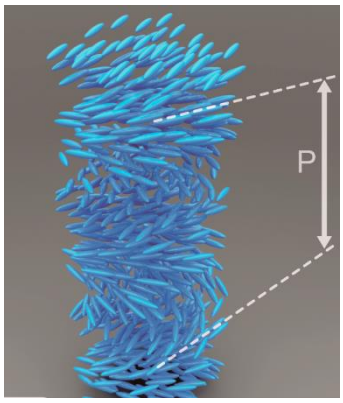

Figure 1.4 - Scheme of the cholesteric LCP in a continuous environment [27].

Solutions of highly anisometric molecules that are stiff enough could form a liquid crystal phase under certain conditions. Cellulose, a long chain of molecules with limited flexibility, meets these requirements and is likely to form liquid crystalline phases. [17,18,19]

Cellulose and its derivatives can form chiral nematic phases, which are liquid crystals with a helicoidal structure. Two main parameters define these phases, the pitch or the distance required for the director (a vector representing the average orientation of the molecules) to rotate 360 degrees along the optical axis and the sense of the helical structure. An LCP was first observed in a cellulosic system in 1976 when vivid colours that altered with the observation angle were observed in a solution of HPC in water. These materials also displayed birefringence, the ability to split light into two distinct rays, and optical activity. [8,10,17,20]

Several factors can affect the pitch and handedness of a cholesteric helix, including temperature, the chemical structure of the side chain, and the degree of polymerization. It was observed that the pitch increases with temperature in HPC cholesteric liquid crystals for molecular weights over 60 000 g/mol. [21]

Cellulose nanocrystals suspensions can form cholesteric chiral nematic phases, indicating that LC cellulosic phases can be produced at different length scales. [17,22,23] In this case, the director rotates from right to left, as represented in Figure 1.4. The concentration of CNCs in suspension affects the pitch value, which decreases with the increase of CNCs concentration [16]. The cholesteric phase of the CNCs presents birefringence [24], allows the selective reflexion of circular polarized light on the left channel and the transmission of CPL on the right one [16]. The interaction of light with the cholesteric phase depends on the value of the mesophase pitch, wavelength, polarization and direction of light propagation, and the change in the refractive index that occurs along the helical axis is responsible for the selective LCP reflection, that is, with the same sense as the cholesteric structure [24, 25]. The maximum reflected wavelength can be described by the de Vries equation (Equation 2), with λ being the maximum reflected wavelength, *n* the average refractive index, *P* the pitch value and θ the angle between the incident light and the helical axis [24, 25].

$$\lambda = n\,P\cos\theta \qquad \text{(Equation 2)}$$

The maximum reflected wavelength varies with the observation angles, translating to the iridescence of the cholesteric structure. The birefringence of the cellulose cholesteric phases can be observed between crossed polarizers [25, 26]. However, the pitch values of the cholesteric structure of CNCs suspensions is typically on the order of micrometres (greater than 1 μm), while the wavelength of visible light is on the order of sub-micrometres (less than 1 μm)., therefore diluted suspensions (3-15% wt) of CNCs do not allow the reflection of light in the visible region. [25]

1.4 Cellulosic solid films

Shear-casting is a technique used to produce films with anisotropic properties from cellulose-based liquid crystalline systems. The films produced through this process have different mechanical characteristics depending on the direction they are stretched. When stretched perpendicular to the

direction of the applied shear force, the films are ductile, while they are brittle when stretched in the direction parallel to the shear force. This anisotropic behaviour is due to the alignment of the cellulosic chains after the shear stress is removed, which is caused by solvent's evaporation, and the chains' high viscosity. The internal stress resulting from the relaxation of the shear-aligned chains leads to a periodic contraction, often referred to as bands, that can be observed in the film. The specific characteristics of the bands, including their composition, thickness, and size, depend on various factors such as the solvent evaporation rate, film thickness, and the duration and intensity of the applied shear force. Corrugations can also be observed in insect wings and in plant petals, such as *Hibiscus trionum* and black tulip. [28, 29, 30]

In the case of flower petals, the diffraction gratings are created by the regular nanoscale patterns (striations or wrinkles) on the surface of the petals, which are moulded into the cuticle that coats the surface of the flat epidermis of the petal. These striations act as diffraction grating because they are closely spaced and parallel to each other, which means that when light strikes the petal's surface, it is dispersed into its different wavelengths creating an iridescent or colourful effect. [28]

2

MATERIALS AND METHODS

2.1 Preparation of CNC suspensions

The aqueous colloidal suspension of nanocrystalline cellulose used in this dissertation is of commercial origin (CelluForce NCC® NCV100-NAL90, Lot nº C1A21019), and a mother suspension of 6.0% wt was produced with it.

The CNCs mother suspension was diluted in type II ultrapure water (*Millipore Elix Advantage 3* water purification system) to obtain suspensions with concentrations: 1.0; 3.5% wt. The diluted solutions were sonicated with an Ultrasonic Processor (UP400St, from Hielscher with a titanium tip with a diameter of 3 mm, 24 KHz, amplitude 80% and pulsed cycle of 30%), under a water bath (to prevent overheating). The energy applied to each suspension was 265.68 kJ/g CNCs.

After sonication, which destroys aggregates and promotes greater fluidity in the suspension and, consequently, promotes phase separation at the macro and micro scale, the suspension was vacuum filtered with a 50 μm filter, with the aid of a vacuum pump (Edwards xDS 5) and subsequently filtered with a syringe with a 1.6 μm filter. Finally, the suspensions were placed in glass bottles at room temperature without exposure to light.

2.2 Preparation of HPC solutions

Four HPC solutions were prepared (M_n= 100,000.0 g/mol, lot A20x013, *Alfa Aesar*) diluted in type II ultrapure water (*Millipore Elix Advantage 3* water purification system), with different concentrations: 50.0; 55.0; 60.0; 65.0 % wt. Subsequently, the solutions were left to rest without exposure to light and were mixed once a day for approximately two weeks.

2.3 CNC/HPC films

The CNC films were produced by drop casting approximately 9.0 g of CNC aqueous suspensions were deposited in petri dishes allowing the solvent to evaporate, at room temperature for approximately

two weeks. After complete evaporation of the solvent, solid CNC films were stored at room temperature for further characterization.

The HPC films were obtained using the shear-casting technique, with a film speed of 1.0 mm/s and a calibrated ruler. These films were deposited on a sheet of parafilm, which was later removed. The thin transparent cellulosic films were obtained by preparing a banded film of HPC atop an iridescent CNCs film. HPC films only, and CNCs+HPC, were obtained for the different HPC concentrations.

Finally, the films obtained from CNCs, HPC and CNCs+HPC were cut into 15x5 mm samples, with the help of the Zmorph VX printer with a class 4 laser head and the Voxelizer 3 program, to be characterized later.

2.4 Collection and preparation of *Xylocopa violacea* wings

Initially, several insects were collected, whose wings exhibit characteristics similar to those of *Xylocopa violacea*. All the insects collected were found already dead in several locations.

After selecting the insect, we decided to study, *Xylocopa violacea*, the species and genus of the various samples was confirmed by Dr. Roberto Keller, Curator of Arachnid and Myriapoda Entomology at the National Museum of Natural History and Science.

The wings of all *Xylocopa violacea* collected were removed from the body, with the aid of scissors, to later be characterized.

2.5 Characterization techniques

Several characterization techniques were carried out to obtain information about the cellulosic materials produced and the *Xylocopa violacea* wings collected, such as polarized optical microscopy (POM), scanning electron microscopy (SEM), visible spectroscopy (VS), uniaxial mechanical tensile tests, thickness, and macroscopic photographs.

3

RESULTS AND DISCUSSIONS

The primary objective of this dissertation was to fabricate cellulose nanocrystal films that exhibit non-iridescent behaviour at specific angles, thereby emulating the structural characteristics observed in the wings of particular insects, notably the *Xylocopa violacea*, Figure 3.1. It is worth noting that CNC films typically display iridescence in the scientific literature, Figure 3.2a. Conversely, films composed of hydroxypropyl cellulose possess a structured surface that restricts light reflection to specific angles due to their corrugated nature.

To address this, the approach involved the production of a CNC film with an overlaid deposition of an HPC film, Figure 3.2b. This stratagem aimed to modify the transparency and iridescence characteristics of the films, specifically targeting angles that replicate the optical properties observed in the wings of the aforementioned insects. A comprehensive characterization process was carried out for both the fabricated films and the insect wings, yielding crucial data for the study's research objectives.

Figure 3.1 - Photograph image of *Xylocopa violacea* with close section of its wing.

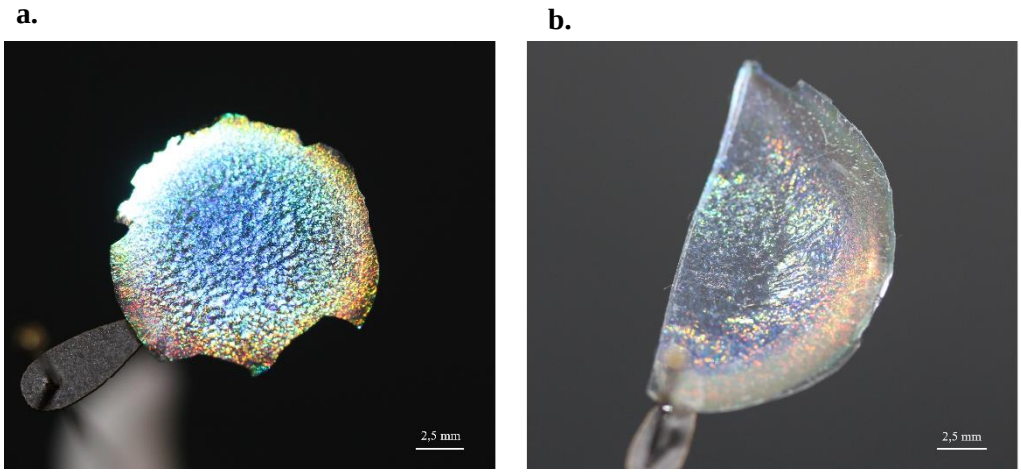

Figure 3.2 - Photographs of **(a)** CNCs film **(b)** CNCs+HPC film.

After the examination of CNC films produced with a 3.5% wt concentration, it was determined that the average thickness was excessively large (~200 μm). Consequently, the decision was made to reduce the CNCs concentration to 1.0% wt. As a result, films with a more suitable thickness were successfully obtained (~60 μm). Following the preparation and microscopic observation, the decision was also made to focus our in-depth study specifically on the HPC films at a concentration of 55% wt. This concentration produced better results, since the thicknesses of the films produced were in the same order of magnitude as the *Xylocopa violacea*'s wings, allowing a more detailed examination of the distinct ripples present in the HPC layer.

3.1 Characterization of the thin films and *Xylocopa violacea* wings

3.1.1 Polarized optical microscopy

The POM images were acquired with an Olympus DP73 camera coupled to an Olympus BX51 polarized light optical microscope connected to a Scott KL2500 light source and using the Olympus Stream Basic 1.9 software.

Images of the central portions of films and wings were captured with crossed polarizers. In the case of the CNC films in Figure 3.3b, it was possible to observe birefringence and the characteristic texture of the cholesteric structure of CNCs. This texture includes the presence of bands retained on a micrometre scale, which were observed in parallel with the surface of the membrane.

In the HPC films in Figure 3.3a and in CNC+HPC films in Figure 3.3d, the distinct bands formed by the HPC film were clearly observed with sharpness. These bands, characterized by their well-defined and prominent features, represent the inherent structural attributes of the HPC layer.

In Figure 3.3c, we can observe that the corrugations seen in the wing membrane are similar to the banded texture observed for the produced from CNCs+HPC. The banded texture represents the sinusoidal modulation of the director along the shear direction This modulation translates into dark and

white bands between cross polarizers corresponding to positions of the director parallel and perpendicular to one of the polarizers.

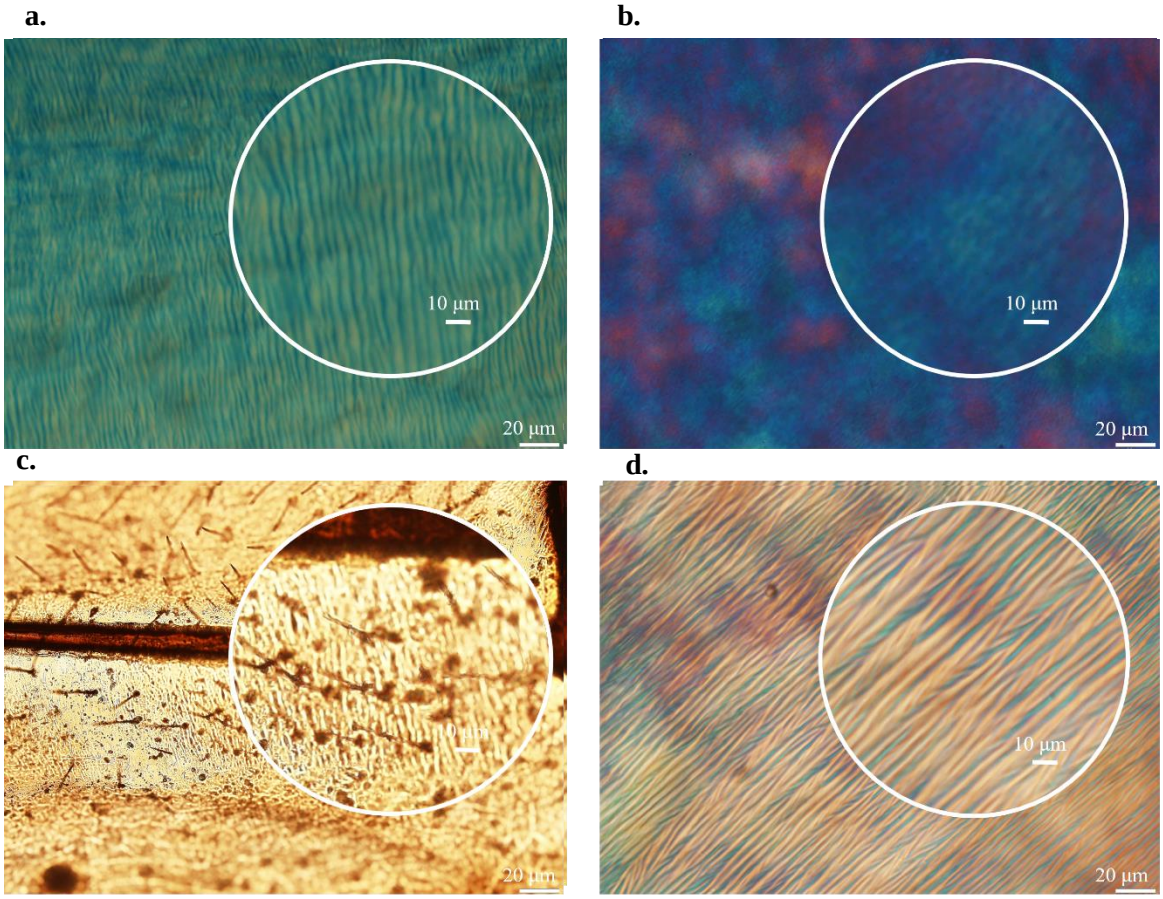

Figure 3.3 – Polarized optical microscopy images of **(a)** HPC film **(b)** CNCs film **(c)** *Xylocopa violacea's* wings **(d)** CNCs+HPC film.

3.1.2 Scanning electron microscopy

SEM images were obtained using *Regulus 8220 Scanning Electron Microscope*. The samples were glued to an aluminium substrate with double-sided carbon tape and coated with an 11.9 nm thin iridium layer (Q150T ES Quorum Sputter Coater). The images were captures in SE(U) mode with 3 kV acceleration voltage and at various magnifications.

The SEM images were obtained through a cross-sectional cut and provided a high-resolution view of the structure and organization of the wings of *Xylocopa violacea* (Figure 3.4a, b, c), allowing for a detailed comparison with the CNC+HPC films (Figure 3.4d, e, f).

One of the key objectives in examining the CNCs+HPC films was to assess the adhesion of the HPC layer to the CNCs film. When the film was subjected to freezing in liquid nitrogen and subsequently fractured, it was observed that during the freeze-thaw process (Figure A.3), the HPC film, detached from the CNCs film at specific regions. This detachment process is clearly visible in Figure 3.4d. Nevertheless, this adhesion deficiency was not uniform throughout the entire film, as there were areas

exhibiting significant adhesion, as illustrated in Figure 3.4f. These observations provide valuable insights into the interfacial properties and adhesion characteristics between the CNCs and HPC components within the composite film. To enhance this adhesion, it may be necessary to refine the sample fracture technique or modify the HPC deposition method by incorporating a step for cleaning the CNC films prior to the HPC deposition. To assess the effectiveness of these enhancements, it would be essential to implement them in future research studies. It is possible to discern certain structural resemblances between the wings and the films. The wings feature an outer layer both above and below, akin to the HPC layer above the CNCs, as shown in Figure 3.4b, e. In future studies, it would also be of interest to conduct the same characterizations on films consisting of CNCs with HPC layers on both sides, to validate their resemblance to the wings of *Xylocopa violacea*.

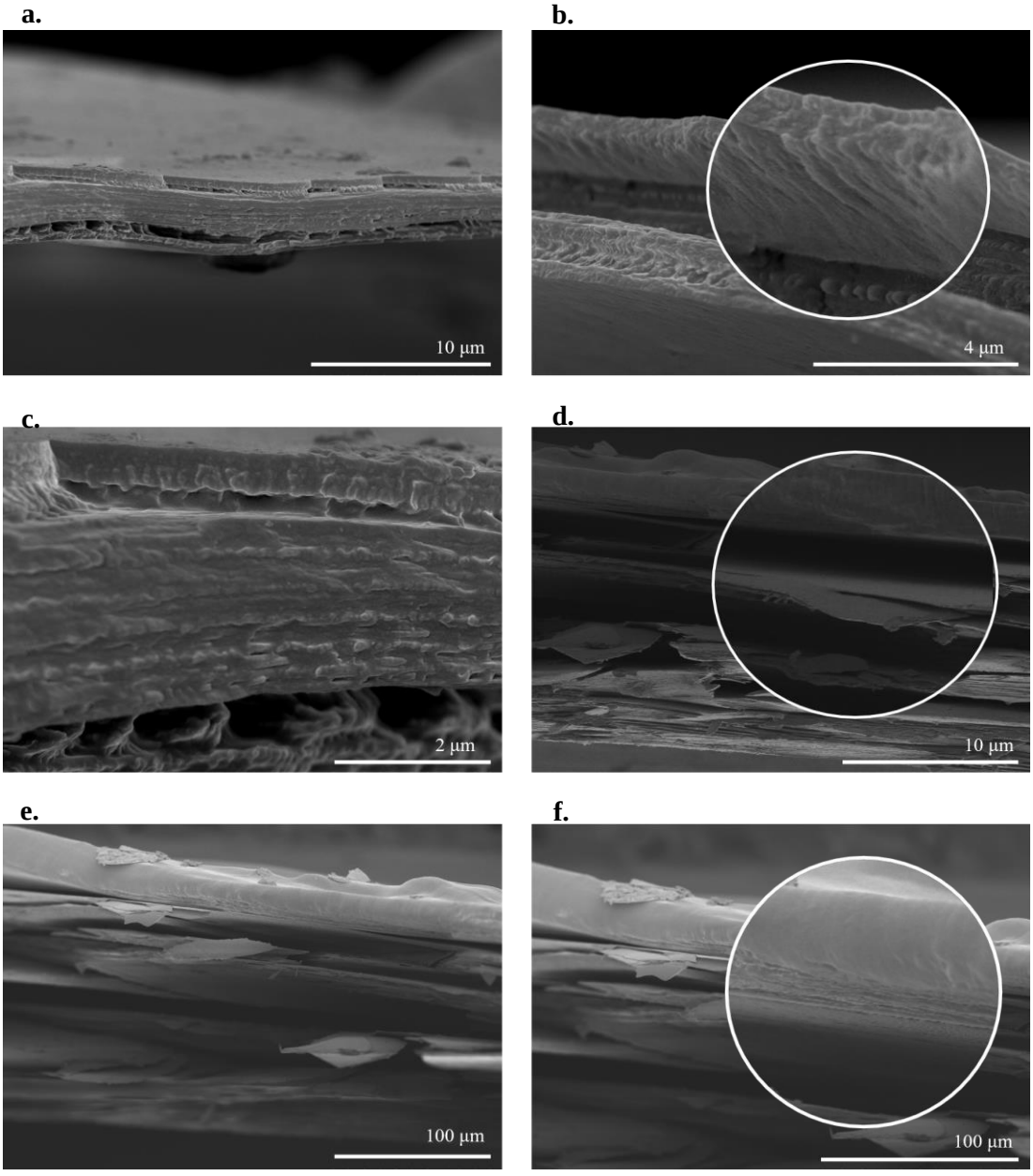

Figure 3.4 - SEM images: **(a), (b), (c)** *Xylocopa violacea's* wings **(d), (e), (f)** CNCs+HPC films

3.1.3 Uniaxial mechanical tensile tests

The average thickness of each CNC, CNC+HPC membrane, each HPC film produced, and each wing was determined with a digital micrometre (Mitutoyo).

Uniaxial mechanical tensile characterization was performed to assess the Young's Module, Yield strength, and tensile strength of the films. For this, a static-dynamic miniature testing machine (*Inspekt micro-LC 100N, Hegewald & Peschke*) was used at a strain rate of 2 mm/min.

To evaluate the films mechanical properties and study the influence of the HPC layer on CNCs films, the samples were submitted to tension tests. For this, each type of sample was submitted to these tests at least three times, with which the statistics of each parameter were calculated.

Before submitting to tension testing using a 20 N load cell at 2 mm/min, the samples were prepared by cutting them into 15x5 mm rectangles. Afterwards, the thickness of each sample was determined.

With the first suspensions of 3.5% wt/wt CNCs prepared, the films obtained were too thick, as can be seen in Figure 3.5a. It was decided to prepare suspensions of 1.0% wt/wt, whose films presented satisfactory thicknesses, since they are similar to those of the wings, Figure 3.5b.

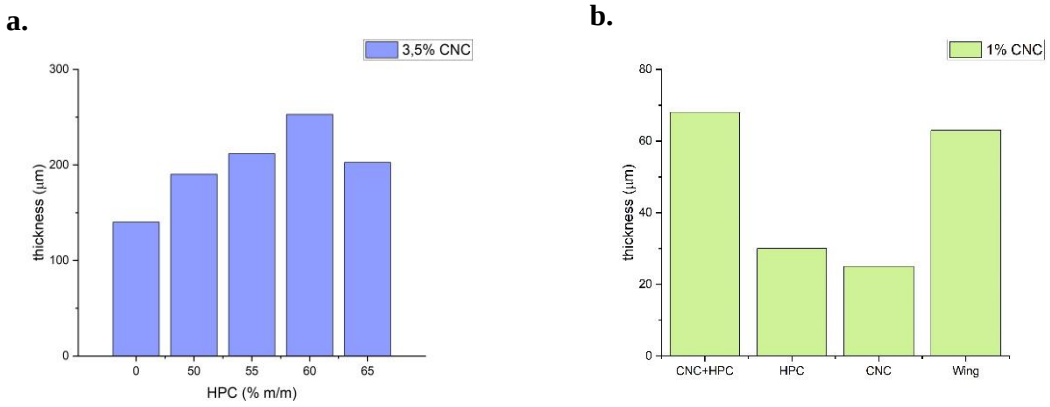

Figure 3.5 - **(a)** thickness for films with 3.5% wt/wt of CNCs **(b)** thickness for films with 1.0% wt/wt of CNCs and 50.0% wt/wt of HPC, and *Xylocopa violacea*'s wings.

The obtained curves for all tested samples, can be observed in Figure 3.6, and the respective parameters in Table 3.1.

Table 3.1 – Average mechanical properties of the tested samples, obtained through tension testing.

Samples	Maximum Stress (MPa)	Yield Stress (MPa)	Maximum Strain	Young's Modulus (MPa)
CNC+HPC (parallel to shear)	16.04 ± 1.32	12.61 ± 1.59	62.15 ± 7.27	0.23 ± 0.0019
CNC+HPC (perpendicular to shear)	15.13 ± 0.23	6.16 ± 0.10	57.48 ± 0.02	0.22 ± 0.0024
HPC (parallel to shear)	33.86 ± 2.93	27.66 ± 0.011	453.26 ± 50.32	0.10 ± 0.047
HPC (perpendicular to shear)	8.01 ± 0.93	8.64 ± 0.49	1006.27 ± 55.39	0.10 ± 0.0044
CNC	330.30 ± 52.2	144.50 ± 10.6	63.08 ± 5.62	0.51 ± 0.048
Wings of *Xylocopa violacea (small)*	29.30	16.50	23.38	0.94
Wings of *Xylocopa violacea (big)*	116.00	101.00	46.18	2.98

The differences between CNC+HPC films oriented parallel and perpendicular to the shear direction exhibit relatively minor distinctions. Notably, a higher Young's modulus and greater strain was observed in the sample oriented parallel to the shear direction. The biggest difference between the two directions was observed in the ultimate stress. In the case of HPC samples, Young's moduli were found to be quite similar; however, the maximum strain was significantly greater in the sample oriented perpendicular to the shear direction. It is worth noting that the addition of the HPC layer dramatically alters

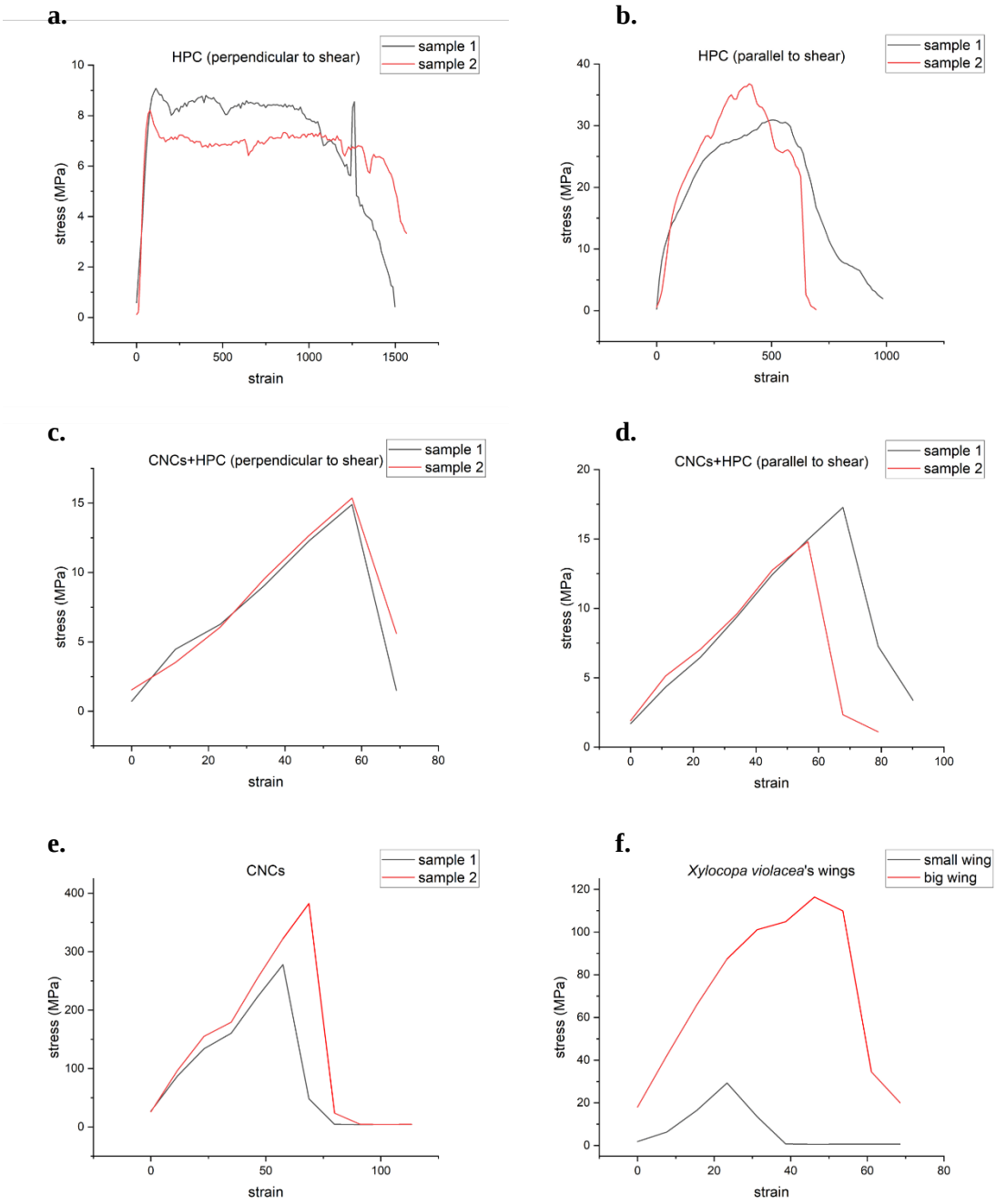

Figure 3.6 - **(a)** stress-strain curves for CNC+HPC parallel to shear samples **(b)** stress-strain curves for CNC+HPC perpendicular to shear samples **(c)** stress-strain curves for HPC parallel to shear samples **(d)** stress-strain curves for HPC perpendicular to shear samples **(e)** stress-strain curves for CNC samples **(f)** stress-strain curves for wings of *Xylocopa violacea* samples.

the Young's modulus. This phenomenon may be attributed to the film's adherence to the grips of the tensile testing machine, a factor that warrants further investigation in more detailed future studies.

Regarding the wings of *Xylocopa violacea*, tests were conducted on both pairs of the insect's wings since it possesses two sets: smaller wings located on the lower part of the insect and larger wings near the head, as illustrated in Figure 3.1. It is apparent that the smaller wing exhibits a higher Young's modulus compared to the larger wing. This difference may be attributed to the presence of more veins, rendering the smaller wing more resistant.

For a more comprehensive comparison between the films and the wings, an extensive study with a larger number of samples would be necessary to yield more precise and less scattered data. Nevertheless, based on the obtained results, some similarity in terms of Young's modulus can be observed between the CNCs film and the larger wing.

3.1.4 Macroscopic photographs and visible spectrum

In ordered photonic structures, photonic pseudo-bandgaps arise from long-range order correlations, causing them to exhibit iridescent coloration. These pseudo-bandgaps result from constructive interference of light reflected at specific crystalline planes within the lattice, yielding angle-dependent, shifting colours. Conversely, in amorphous photonic structures, photonic pseudo-bandgaps originate from short-range order, leading to noniridescent structural colours. This noniridescence emerges because light is uniformly scattered in all directions, thereby lacking directional discrimination within random or amorphous photonic structures. [31, 32, 33]

The macroscopic photographs of all the membranes and wings of *Xylocopa violacea* were captured with the Leica DMC4500 camera, coupled to the Leica Z6 APO microscope and 1.0x objective, using the Leica Application Suite X 2.0 software. The reflection spectrums were obtained with the Sarspec spectrometer using the LightScan 2.0 software.

To assess the effectiveness of the HPC layer in altering iridescence at specific angles, visible spectra were acquired from the produced films and wings (Figure 3.8, Figure 3.9, Figure 3.10), along with corresponding photographs (Figure 3.7) for specific angles.

The acquired spectra exhibit significant differences in intensity concerning the angle but show minimal variations in terms of wavelength. When considering the visible spectrum range of 360-720 nm, several observations can be made: wings display colour reflection over a broader range of angles; CNCs reflect colour within a relatively narrow angle range of approximately 20-degree; the CNCs+HPC film appears to be more selective, reflecting predominantly at a specific angle. Notably, the CNCs+HPC graph at a 20-degree incidence angle does not saturate in the same manner as the wing and CNCs.

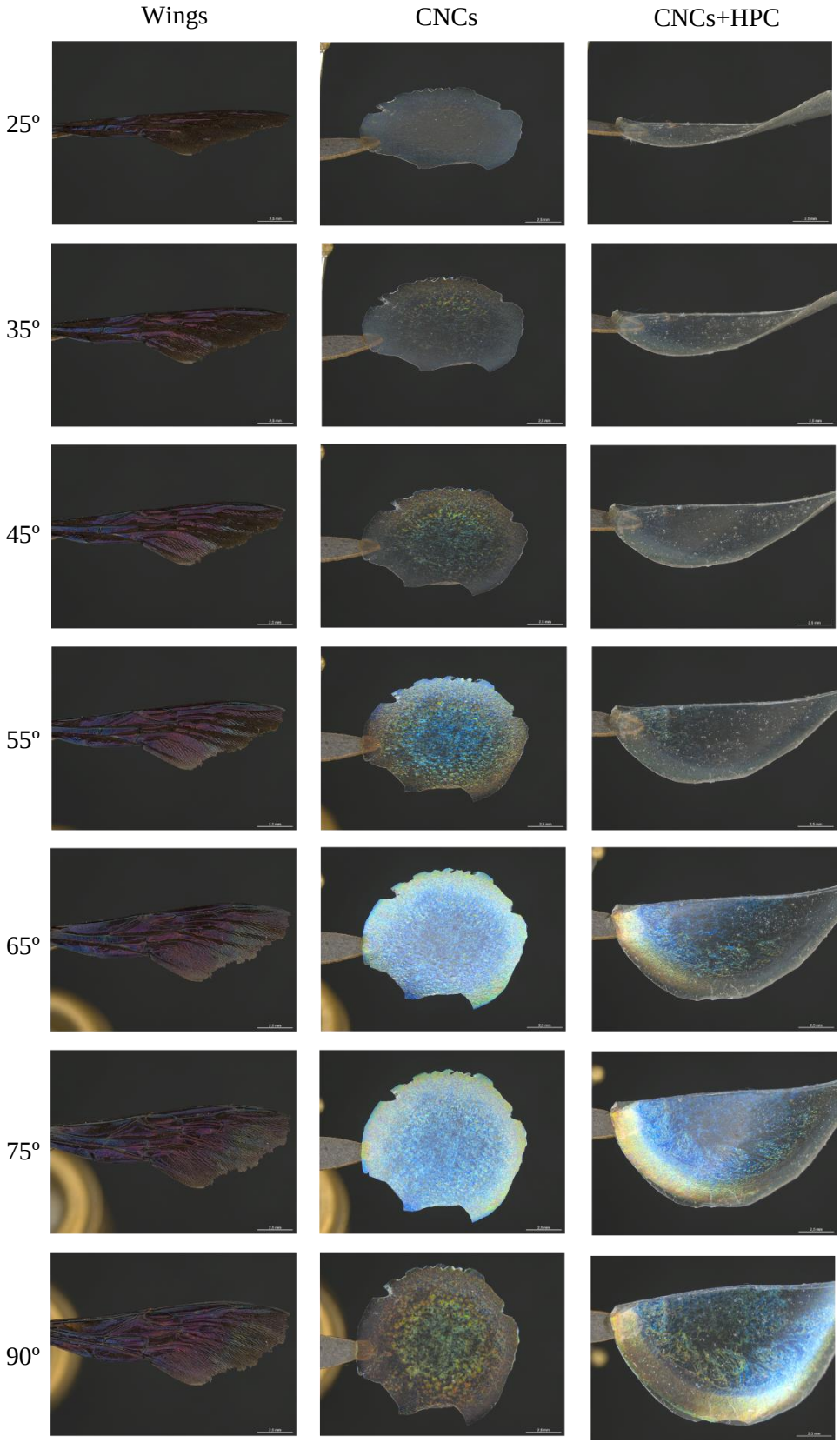

Figure 3.7 - Macroscopic photographs of *Xylocopa violacea*'s wings, CNCs films, CNCs+HPC films, for different angles: 25, 35, 45, 55, 65, 75, 90º.

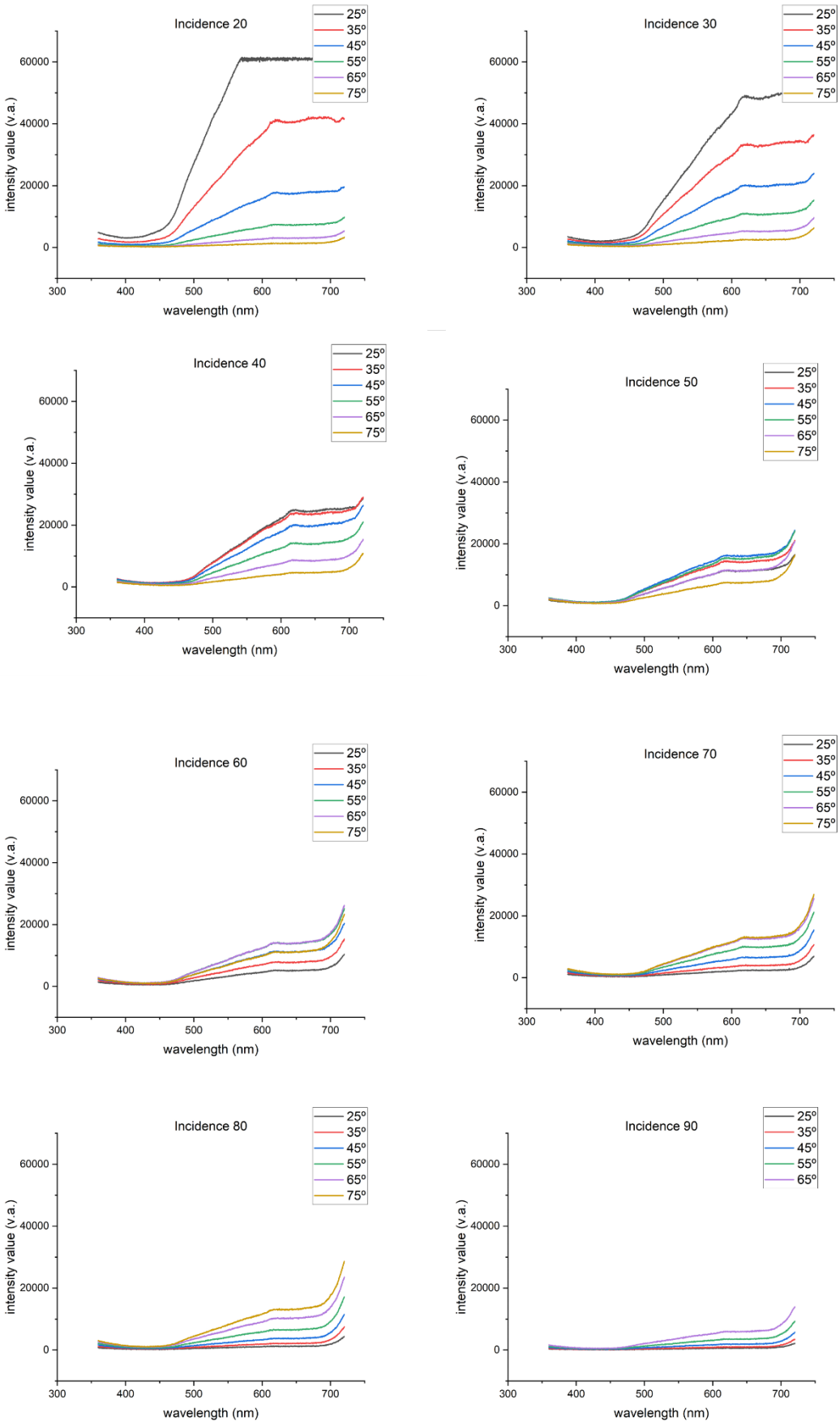

Figure 3.8 - Visible spectrum of *Xylocopa violacea*'s wings for different incidence and detection angles.

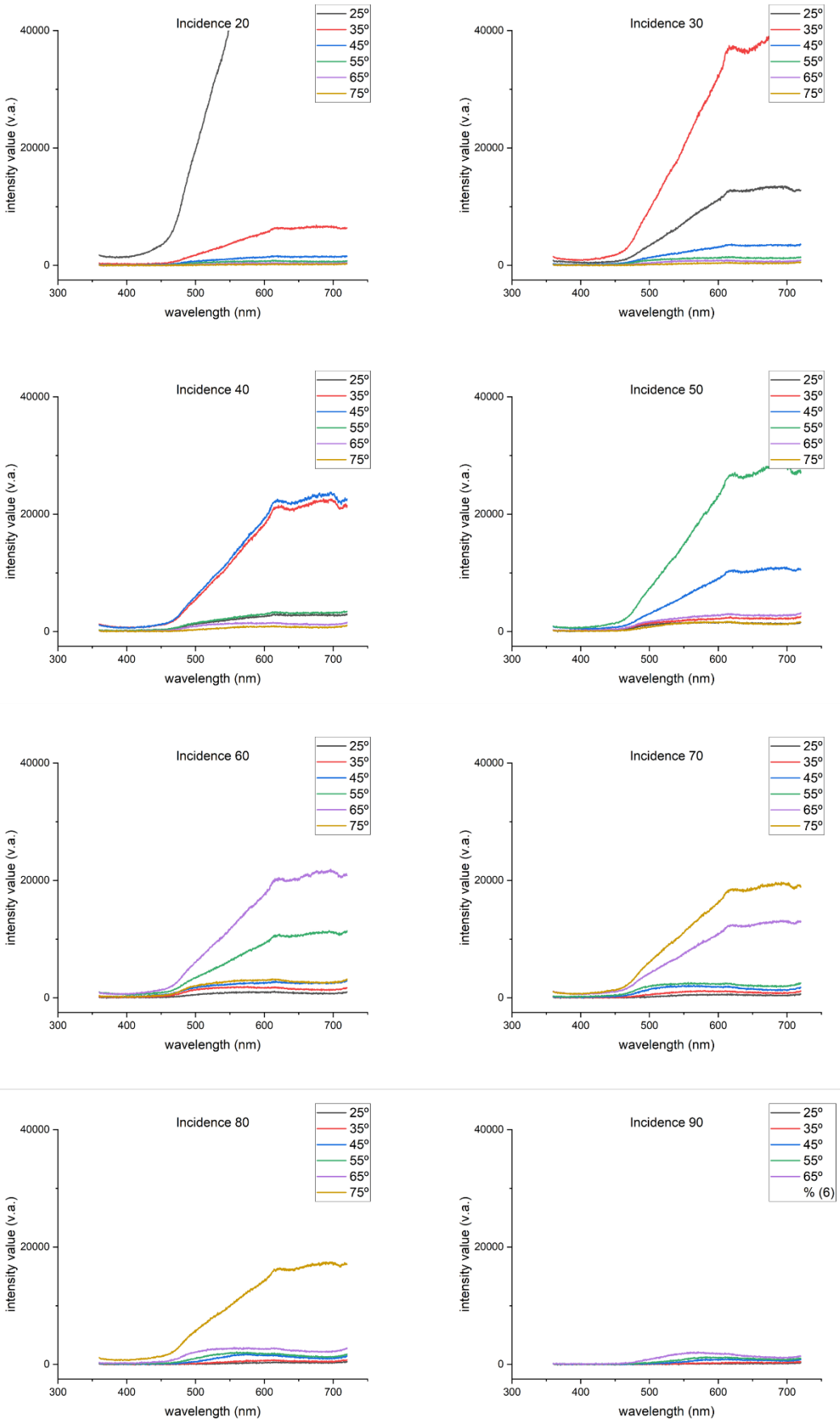

Figure 3.9 - Visible spectrum of CNCs films for different incidence and detection angles.

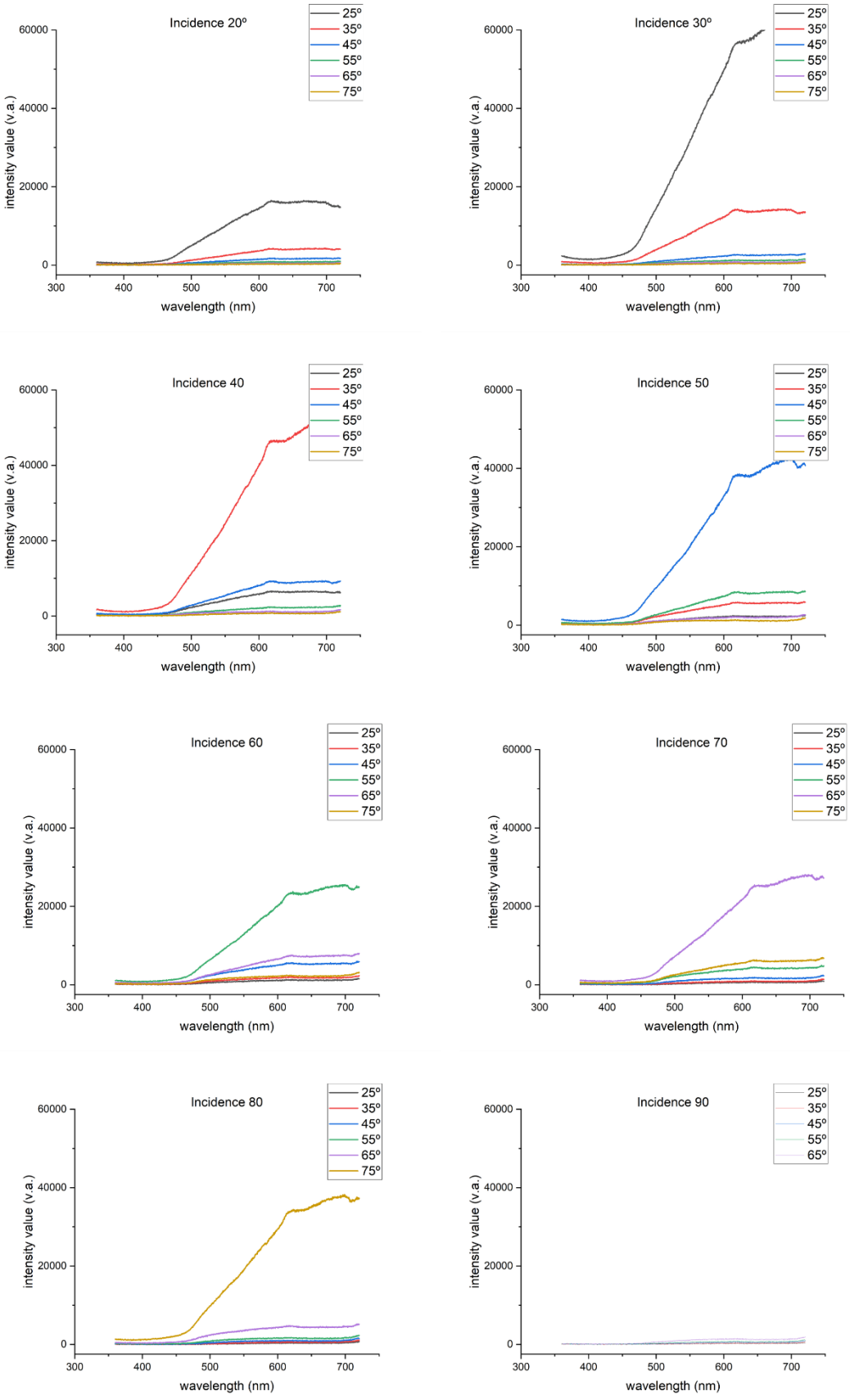

Figure 3.10 - Visible spectrum of CNCs+HPC films for different incidence and detection angles.

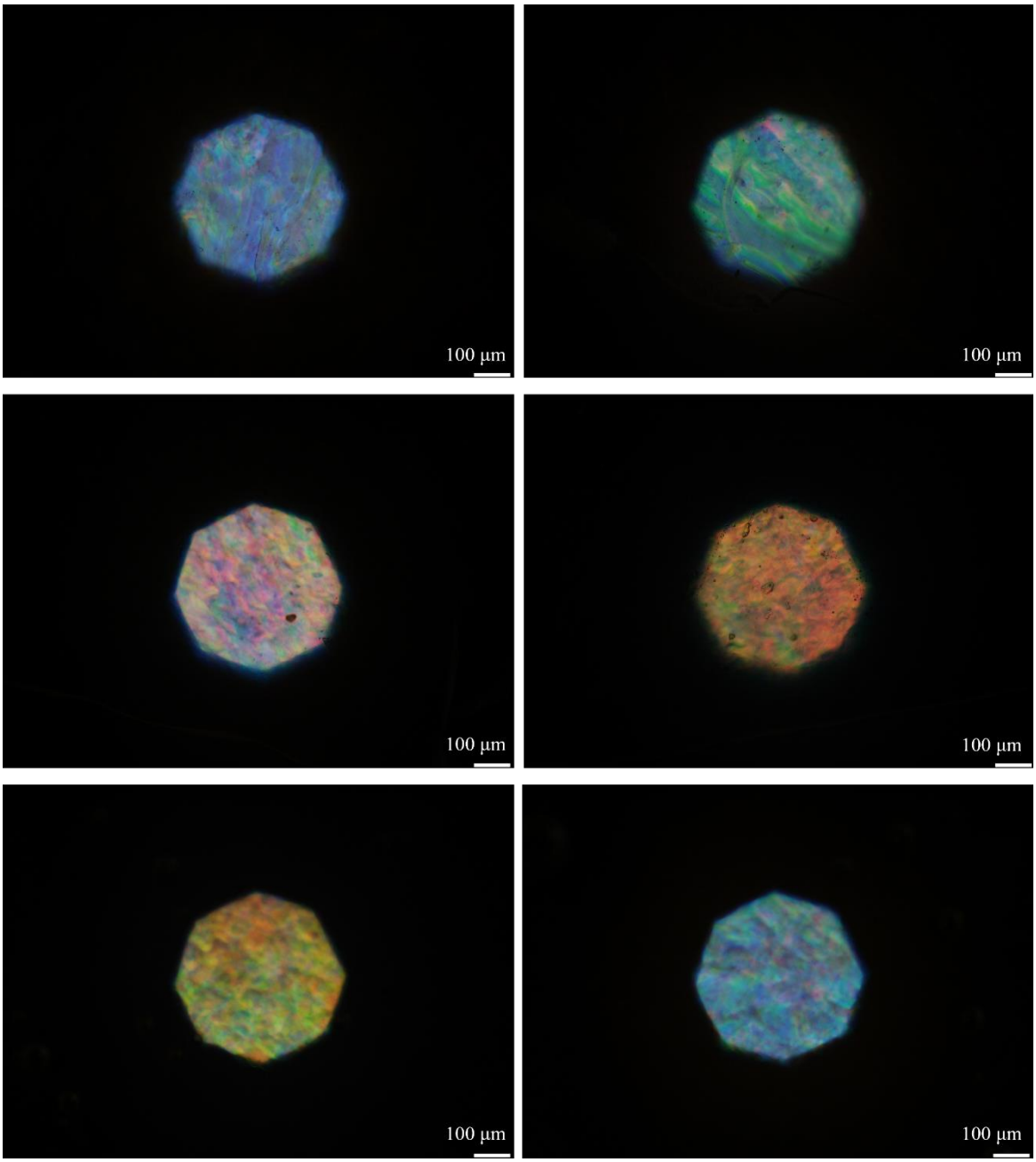

Figure 3.11 - Microscopic images of CNCs film, obtained in reflexion for different angles.

In Figure 3.11, microscopic images of a CNCs film under reflective illumination, with varying angles of incident light and 90° detection, are depicted. These images were captured using an optical microscope, revealing the iridescence of the CNC films due to the wavelength variation with the changing angle of incident light. Notably, these observations preceded those represented in Figure 3.7, ultimately demonstrating different outcomes from those observed under the optical microscope. Consequently, it can be deduced that the findings presented in Figure 3.7 underwent modifications compared to the initial images obtained, a phenomenon that warrants investigation in future studies to elucidate the underlying causes for this discrepancy.

4

CONCLUSIONS AND FUTURE PERSPECTIVES

The primary objective of this dissertation was to create cellulose nanocrystal films that imitate the non-iridescent characteristics observed in the wings of specific insects, particularly the *Xylocopa violacea,* for certain angles. The aim was to produce films that display non-iridescence at certain angles, in contrast to the typical iridescent behaviour associated with CNC films in scientific literature.

This research has achieved significant milestones in the fabrication, characterization, and analysis of cellulose nanocrystal films and their hybrid counterparts with hydroxypropyl cellulose. By reducing the CNC concentration from 3.5% to 1.0% wt, we successfully produced films that closely replicated the structural characteristics observed in the wings of the *Xylocopa violacea*.

The uniaxial mechanical tensile tests provided crucial insights into the structural integrity and behaviour of the CNC and HPC composite films. Through detailed analysis of the Young's modulus and strain, we identified significant correlations between the mechanical properties of the films and the natural structure of *Xylocopa violacea's* wings. These findings underscore the influence of vein structure of the wings on the mechanical behaviour of the bioinspired materials, highlighting potential avenues for further research and development in this domain.

Through the innovative methodology integrating an overlay of HPC onto the CNC films, we effectively manipulated the transparency and iridescence properties, aligning them with the optical features of the insect wings.

The comprehensive characterization employing polarized optical microscopy, scanning electron microscopy, and mechanical tensile tests provided invaluable insights into the structural and mechanical properties of the composite materials. While the spectrometer results did not meet our initial expectations, the POM analysis clearly demonstrated the effect of the HPC layer on the CNC films in terms of altering iridescence for specific angles. Therefore, future studies will require either a repetition of this step or parameter adjustments to ensure the alignment of POM images with the spectral data obtained.

This underscores the importance of continued research and development in refining the correlation between the observed optical properties and the spectral data, highlighting the necessity for improved synchronization between different characterization techniques. These efforts are crucial for enhancing the overall understanding and application of bioinspired materials in the realm of advanced optical and material science.

In essence, this study serves as a significant contribution to the evolving landscape of biomimetic materials, setting the stage for further exploration and refinement in the design and engineering of bioinspired materials for diverse technological applications.

BIBLIOGRAPHY

[1] Whitney H., Kolle M., Andrew P., Chittka L., Steiner U., Glover B., Iridescence, Produced by Diffractive Optics, Acts As a Cue for Animal Pollinators, Science, 323, 130, 2009.

[2] Shevtsova E., Hansson C., Janzen D., Kjærandsen J., Stable structural color patterns displayed on transparent insect wings, PNAS, 108(2), 668, 2011.

[3] Godinho M.H., Fonseca J.G., Ribeiro A.C., Melo L.V., Brogueira P., Atomic force microscopy study of hydroxypropyl cellulose films prepared from liquid crystalline aqueous solutions, Macromolecules, 35, 5932, 2002.

[4] Peter J. Collings. (2002). 2nd ed. Liquid Crystals: Nature's Delicate Phase Of Matter.

[5] Credou J, Berthelot T (2014) Cellulose: from biocompatible to bioactive material. J Mater Chem B 2(30):4767–4788

[6] Klemm D, Heublein B, Fink HP, Bohn A (2005) Cellulose: fascinating biopolymer and sustainable raw material. Angew Chem 44(22):3358–3393

[7] Perez S, Mazeau K (2005) Conformations, structures, and morphologies of celluloses. In: Dumitriu S (ed) Polysaccharides structural diversity and functional versatility, 2nd edn. Marcel Dekker, New York, pp 41–68

[8] de Gennes PG, Frost J (1993) The physics of liquid crystals, 2nd edn. Oxford University Press, Oxford.

[9] Robert J. Ouellette, J. David Rawn. Organic Chemistry (Second Edition), Academic Press, Pages 889-928, (2018). Doi: 10.1016/B978-0-12-812838-1.50028-1.

[10] Werbowyj RS, Gray DG (1976) Liquid crystalline structure in aqueous hydroxypropyl cellulose solutions. Mol Cryst Liq Cryst 34(4):97–103

[11] Shimamura K, White JL, Fellers JF (1981) Hydroxypropylcellulose, a thermotropic liquid crystal: characteristics and structure development in continuous extrusion and melt spinning. J Appl Polym Sci 26(7):2165–2180

[12] Wustenberg T (2014) Hydroxypropylcellulose. In: Wustenberg T (ed) Cellulose and cellulose derivatives in the food industry. Wiley, Weinheim, pp 319–342

[13] Singh S, Dunmur DA (2002) Liquid crystals: fundamentals. Liquid crystals: physical properties and nonlinear, Ed. World Scientific Publishing Co. ISBN 9810242506.

[14] J. A. Kelly, M. Giese, K. E. Shopsowitz, W. Y. Hamad, e M. J. MacLachlan, «The development of chiral nematic mesoporous materials», Acc. Chem. Res., vol. 47, n. 4, pp. 1088–1096, 2014, doi: 10.1021/ar400243m.
[15] B. Thomas et al., «Nanocellulose, a Versatile Green Platform: From Biosources to Materials and Their Applications», Chem. Rev., vol. 118, n. 24, pp. 11575–11625, Dez. 2018, doi: 10.1021/acs.chemrev.7b00627.
[16] D. V. Saraiva et al., «Flexible and Structural Coloured Composite Films from Cellulose Nanocrystals/Hydroxypropyl Cellulose Lyotropic Suspensions», Crystals, vol. 10, n. 2, p. 122, Fev. 2020, doi: 10.3390/cryst10020122.
[17] S.N. Fernandes et al. (2015) Functional Materials from Liquid Crystalline Cellulose Derivatives: Synthetic Routes, Characterization and Applications. Liquid Crystalline Polymers, DOI 10.1007/978-3-319-20270-9_14
[18] Flory PJ (1956) Statistical thermodynamics of semi-flexible chain molecules. Proc R Soc A Math Phys Eng Sci 234:60–73
[19] Gray DG (1983) Liquid crystalline cellulose derivatives. J Appl Polym Sci Appl Polym Symp 37:179–192
[20] De Vries H (1951) Rotatory power and other optical properties of certain liquid crystals. Acta Crystallogr 4(3):219–226
[21] Charlet G, Gray DG (1987) Solid cholesteric films cast from aqueous (hydroxypropyl)cellulose. Macromolecules 20(1):33–38
[22] Sugiyama J, Okano T, Yamamoto H, Horii F (1990) Transformation of Valonia cellulose crystals by an alkaline hydrothermal treatment. Macromolecules 23(12):3196–3198
[23] Fleming K, Gray DG, Matthews S (2001) Cellulose crystallites. Chem Eur J 7:1831–1835
[24] W. Hong, Z. Yuan, e X. Chen, «Structural Color Materials for Optical Anticounterfeiting», Small, vol. 16, n. 16, pp. 1–25, (2020), doi: 10.1002/smll.201907626.
[25] R. M. Parker et al., «The Self-Assembly of Cellulose Nanocrystals: Hierarchical Design of Visual Appearance», Adv. Mater., vol. 30, n. 19, p. 1704477, Mai. 2018, doi: 10.1002/adma.201704477.
[26] A. P. C. Almeida, J. P. Canejo, S. N. Fernandes, C. Echeverria, P. L. Almeida, e M. H. Godinho, «Cellulose-Based Biomimetics and Their Applications», Adv. Mater., vol. 30, n. 19, p. 1703655, Mai. 2018, doi: 10.1002/adma.201703655.
[27] Recent advances in the manipulation of circularly polarised light with cellulose nanocrystal films, S.N. Fernandes, L.F. Lopes, M.H. Godinho, Current Opinion in Solid State and Materials Science, 23(2), 63, 2019
[28] Ana P. C. Almeida, João P. Canejo, Susete N. Fernandes, Coro Echeverria, Pedro L. Almeida, and Maria H. Godinho, Cellulose-Based Biomimetics and Their Applications, Advanced Materials, 1703655, (2018).
[29] JP Canejo, N Monge, C Echeverria, SN Fernandes, MH Godinho, Cellulosic liquid crystals for films and fibers, Liquid Crystals Reviews, 5 (2), 86-110, (2018).

[30] C Echeverria, PL Almeida, JL Figueirinhas, MH Godinho, Understanding the influence of carbon nanotubes on the flow behavior of liquid crystalline hydroxypropylcellulose: A Rheo-NMR study, Polymer, 180,121675, (2019).
[31] Freymann, G. von, Kitaev, V., Lotsch, B. V. & Ozin, G. A. Bottom-up assembly of photonic crystals. Chem Soc Rev. 42, 2528–2554 (2013).
[32] Dong, B. Q., Liu, X. H., Zhan, T. R., Jiang, L. P., Yin, H. W., Liu, F. & Zi, J. Structural coloration and photonic pseudogap in natural random closepacking photonic structures. Opt. Express 18, 14430–14438 (2010).
[33] Saranathan, V., Forster, J. D., Noh, H., Liew, S.-F., Mochrie, S. G. J., Cao, H., Dufresne, E. R. & Prum, R. O. Structure and optical function of amorphous photonic nanostructures from avian feather barbs: a comparative small angle X-ray scattering (SAXS) analysis of 230 bird species. J. R. Soc. Interface 9, 2563–2580 (2012).

A

APPENDIX - A

A.1 Images

Figure A.1 - Different angles of *Xylocopa violacea*'s wings.

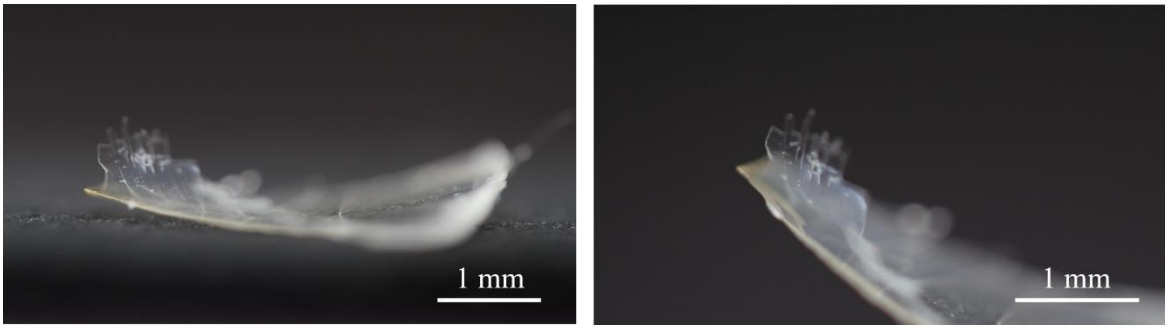

Figure A.3 - CNCs+HPC film during freeze-thaw process.

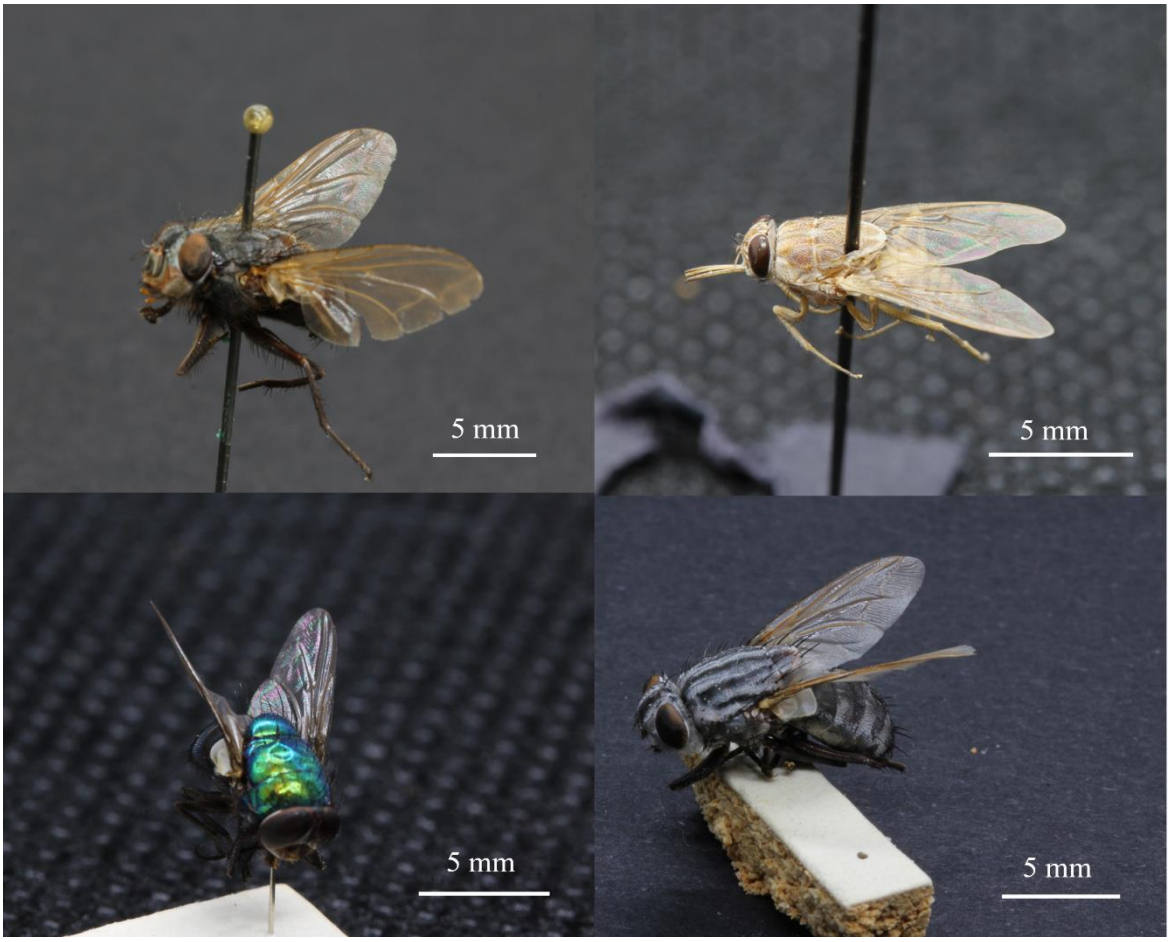

Figure A.2 - Different insects studied, before choosing *Xylocopa violacea's*.

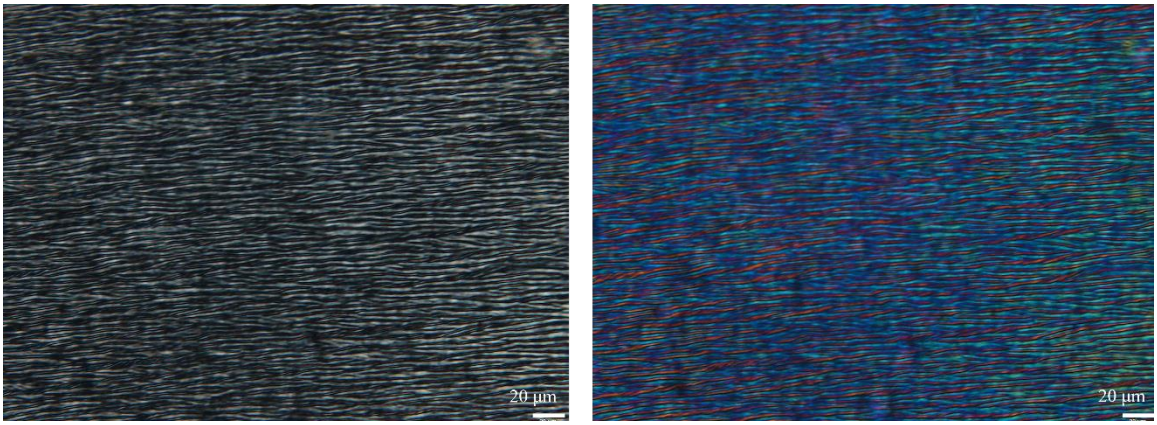

Figure A.4 – HPC solid film banded structure observed by POM in transmission, under cross polarizers, on the left, and under cross polarizers and a lambda plate, on the right.